Comparison of implicit, explicit, center and upwind schemes for the simulation of internal vortex flow at low Mach number

Marc Buffat[1] Anne Cadiou [2]
Lionel Le Penven [2] Catherine Le Ribault[2]

[1]UCB Lyon I, LMFA UMR 5509

[2]CNRS, LMFA UMR 5509

Low Mach Conference (Porquerolles) June 2004

Outlines

Motivation

- Motivation: tumble flow in reciprocating engine

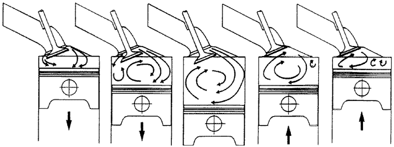

Numerical difficulties

- Low Mach with different time scales (slow and fast)
- Different scaling of the state variables: $\rho = \theta(1)$, $u = \theta(1)$, $p = \theta(Ma^{-2})$
- CFL stability condition based on c (celerity), not u (velocity)

Model flow

Model

Taylor Vortex in a square cavity

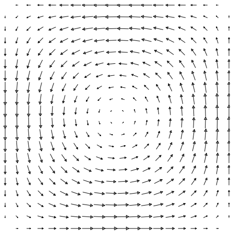

Internal vortex flows at Low Mach

1. Inviscid case:
   asymptotic analysis,
   slow time density fluctuation $\theta(Ma^2)$
   fast time pressure fluctuation $\theta(Ma^3)$
2. Viscous decay:
   numerical dissipation (order)
3. Compression effect:
   2D flow
   3D perturbed flow (elliptical instability)

Numerical schemes

Conservation equations for $W = \left[\rho, \rho\vec{U}, E = \frac{p}{\gamma-1} + \frac{1}{2}\rho U^2\right]$

$$\frac{\partial W}{\partial t} + \underbrace{div\left(\mathcal{A}(W)W\right)}_{\text{Euler flux}} = \underbrace{div\left(\mathcal{R}(W)\right)}_{\text{viscous flux}} + \underbrace{\mathcal{S}(W)}_{\text{source}}$$

Numerical difficulties: Euler flux $\mathcal{F}(W) = \mathcal{A}(W)W$

Explicit scheme with a stability condition $CFL < 1$

- Explicit 2nd order centered scheme: unstable
- Upwind explicit scheme (using the eigenvalues of $\mathcal{A}$)
- High order explicit scheme (i.e. >2)

Implicit scheme $CFL > 1$

- Implicit non linear centered scheme

NadiaLES code

- Explicit mixed FE/FV with LES model on unstructured 3D mesh (Duchamp 1999)

- FV/FE on unstructured mesh (Dervieux 1998)

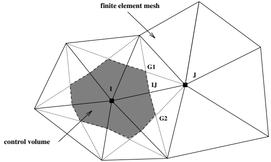

- Low Mach Riemann solver Roe-Turkel (Viozat 1997)
- Control of dissipation and dispersion

- Precision $O(dt^4, h^2)$ with Runge Kutta 4
- Domain decomposition (//e with MPI)

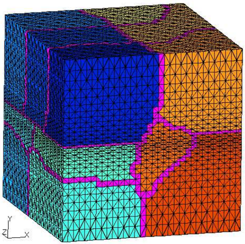

NadiaDF code

- 2D/3D explicit F.D. code with 2 high order schemes on structured mesh

PADE: Lele 1992

reconstruction of the derivative at order 4

$$\alpha F'_{i-1} + F'_i + \alpha F'_{i+1} = a \frac{F_{i+1} - F_{i-1}}{2\Delta x}$$

with $\alpha = \frac{1}{4}$, $a = \frac{4}{3}$
$\rightsquigarrow$ tri-diagonal system (Thomas)

WENO: Jiang & Shu 1996

reconstruction of the fluxes at order 5

$$F_{i+\frac{1}{2}} = \sum_{r=0}^{2} \omega_r F^{+,r}_{i+\frac{1}{2}} + \sum_{r=0}^{2} \omega_{2-r} F^{-,r}_{i+\frac{1}{2}}$$

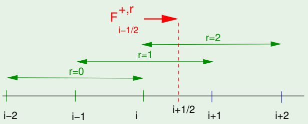

NadiaVF code

- 2D/3D parallel implicit FV on unstructured mesh (written in C++)

- Non linear implicit BDF

$$\frac{3W^{n+1} - 4W^n + W^{n-1}}{2\Delta t} = F(W^{n+1})$$

- Newton $G(W^{n+1}) = 0$

$$\left(\frac{\partial G}{\partial W}\right)_k (W_{k+1}^{n+1} - W_k^{n+1}) = G(W_k^{n+1})$$

- Centered FV of order 2

$$\overline{\frac{\partial W}{\partial x_i}} = \frac{1}{V_k}\int_{\Gamma_k} W\, n_i\, d\Gamma$$

- LibMesh (Kirk 2002)
  FE mesh in //e (C++) with
  non conform grid
  adaptation (AMR)
- PETSC (Barry 2001)
  //e solution of linear system
  Krilov, Multi-Grid
- METIS (Karypis 1996)
  domain partitioning

Preconditioning at low Mach

Mach dependance of the state variables

$\rho = \theta(1)$ and $u = \theta(1)$ but $E = \theta(Ma^{-2})$ and $p = \theta(Ma^{-2})$

NadiaLES

Roe-Turkel (Viozat 1999)

- preconditioning of Δp (β^2)
- entropic variables $[p, \overrightarrow{u}, S]$:

$\beta \approx Ma$

NadiaVF

- decomposition of E and p

$$E(x,t) = \frac{1}{\gamma-1} P_0(t) + E'(x,t)$$
$$p(x,t) = P_0(t) + p'(x,t)$$

- equation for E'

$E'(x,t) = \theta(1)$ and $p'(x,t) = \theta(1)$

with $P_0(t) = \left(\frac{V(0)}{V(t)}\right)^{\gamma} \int_{V(0)} p(x,t)\,dx$

Asymptotic analysis

Initial condition

Taylor vortex with uniform density $\rho_0 = 1$:

$$\overrightarrow{U} = \overrightarrow{U_2(x)} = [\sin \pi x \cos \pi y, -\cos \pi x \sin \pi y],$$

$$P = P_0 + P_2(x) = \frac{1}{\gamma Ma^2} + \frac{1}{4}(\cos 2\pi x + \cos 2\pi y)$$

asymptotic solution

$$\rho(x,t,\tau) = 1 + M_a^2 \rho_2(x,\tau) + M_a^3 \rho_3(x,t,\tau)$$

$$U(x,t,\tau) = U_2(x) + M_a^2 U_4(x,t,\tau)$$

$$P(x,t,\tau) = \frac{1}{\gamma} M_a^{-2} + P_2(x) + M_a P_3(x,t,\tau)$$

Physical solution

steady incompressible part + slow time (τ) part + fast time (t) part

Slow time solution (convection)

At t=0, streamlines $\neq$ isobars $\rightsquigarrow$Fluctuation of density ρ_2

Conservation of entropy $s = s_0 + M_a^2 s_2$ along a trajectory $X(\tau, X_0)$

$\rightsquigarrow \rho_2(X) + \frac{M_a^2}{2} U_2^2(X) = cste = \frac{M_a^2}{2} U_2^2(X_0)$

$\rightsquigarrow \rho_2(X)$ periodic with $T = \frac{T_p}{4}$ ($T_p(X_0)$= travel time along the trajectory)

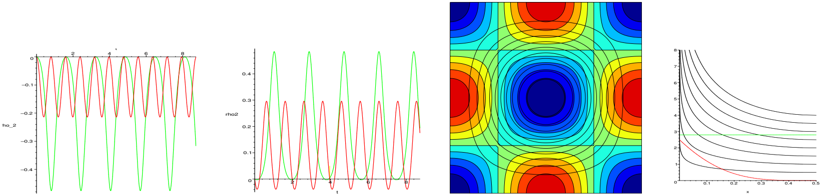

(a) $\rho_2(X)$ (b) $\rho_2(X_0)$ (c) $U_2^2(x,y)$ (d) $\frac{k}{4} T_p$

Figure: $X_0 = [0.2, 0.1]$ ($T_p = 3.95$) and $X_0 = [0.05, 0.025]$

Slow time $\rho_2(X,\tau)$ field

Simulation with FEMLAB (EF P^2) of the transport equation

$$\frac{\partial \rho_2}{\partial \tau} + \vec{U}_2 \vec{\nabla} \rho_2 = -\frac{M_a^2}{2} \vec{U}_2 \vec{\nabla} U_2^2$$

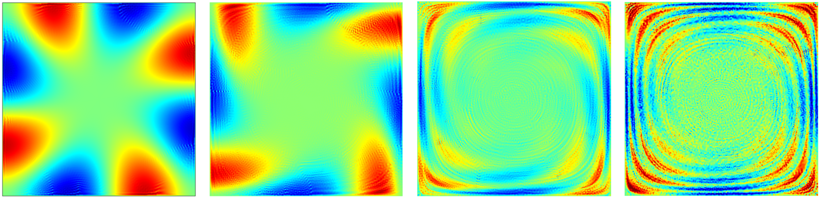

(a) $\tau = 0.1$ (b) $\tau = 0.5$ (c) $\tau = 2$ (d) $\tau = 4$

Figure: $\rho_2(x,y,\tau)$ at different times (ANIMATION)

Fast time solution (acoustic)

The pressure $P_3(x,y,t)$ is solution of a wave equation

$$\frac{\partial^2 P_3}{\partial t^2} - M_a^{-2}\Delta P_3 = 0 \quad \text{with} \quad \frac{\partial P_3}{\partial n} = 0$$

at $t = 0$ $P_3 = 0$, and $\frac{\partial P_3}{\partial t} = M_a f(U_2.\nabla U_2^2)$
$P_3(x,y,t)$ is a combinaison of the acoustic modes of the cavity

$$P_3(x,y,t) = M_a \sum_{p,q=0}^{\infty} P_{pq} \cos p\pi x \cos q\pi y \; e^{I M_a^{-1}\sqrt{p^2+q^2}\pi t}$$

First exited acoustic mode $P_{3,1} - P_{1,3}$ with frequency $f_{3,1} = \frac{\sqrt{10}}{2} M_a^{-1}$

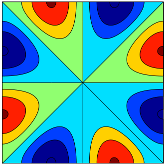

Behaviour of the numerical schemes

Every scheme is able to capture the incompressible solution

CFL	M_a	NadiaVF 0.5	NadiaVF 10	Padé 0.6	Weno 0.6	NadiaLES 0.6
$\|\rho\| - \|\rho_0\|$	0.1	10^{-5}	10^{-5}	-10^{-3}	10^{-4}	$< 10^{-4}$
	0.01	$< 10^{-11}$	$< 10^{-11}$	-10^{-5}	10^{-6}	$< 10^{-4}$
$\|\rho U\| - \|\rho_0 U_2\|$	0.1	-10^{-4}	-10^{-4}	-10^{-3}	-10^{-3}	-10^{-3}
	0.01	-10^{-6}	-10^{-6}	-10^{-4}	-10^{-3}	-10^{-3}

Table: departure from the incompressible solution $\rho = \rho_0$, $U(x,y) = U_2(x,y)$ at time $t = 8.72$ with 80^2

But different behaviours for the prediction of the slow and fast solution

Numerical prediction of the slow part (NadiaVF)

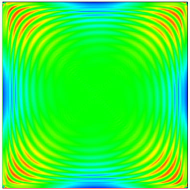

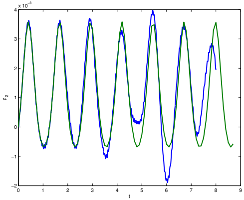

$-0.007 < \rho_2 < 0.007$

$\rho_2(\tau)$ at $X = [0.8, 0.05]$

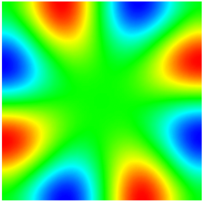

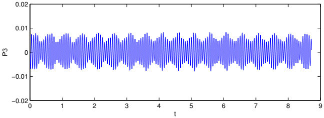

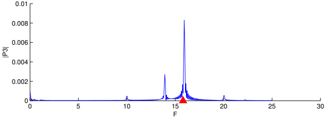

$-0.003 < P_3 < 0.005$

$P_3(t)$at $X = [0.8, 0.05]$

Comparison of the slow part predictions

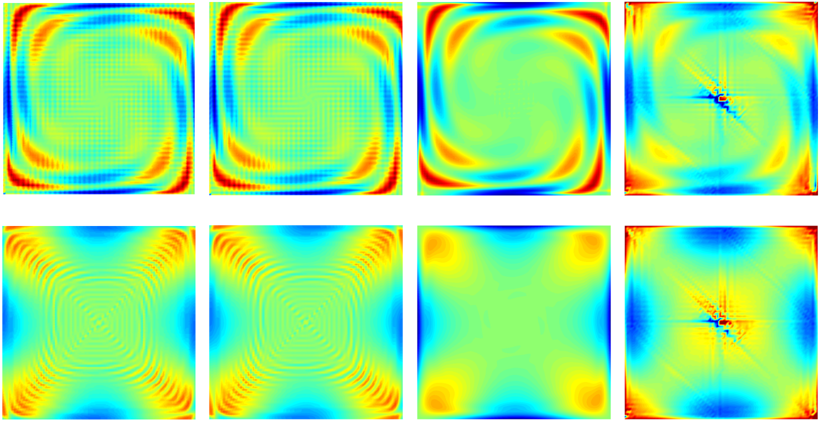

(a) NadiaVF (b) CFL=10 (c) Padé (d) NadiaVF

Figure: Slow part $\rho_2(x,y,\tau)$ at $\tau = 2$ and $\tau = 8.7$ (mesh 80^2)

Comparison of the slow part predictions

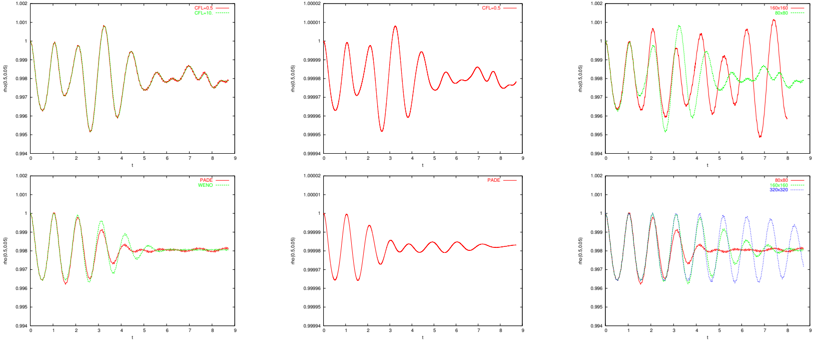

Figure: Slow part $\rho_2(0.5, 0.05, \tau)$: influence of M_a and mesh size with NadiaVF and NadiaDF

Numerical prediction of the acoustic part

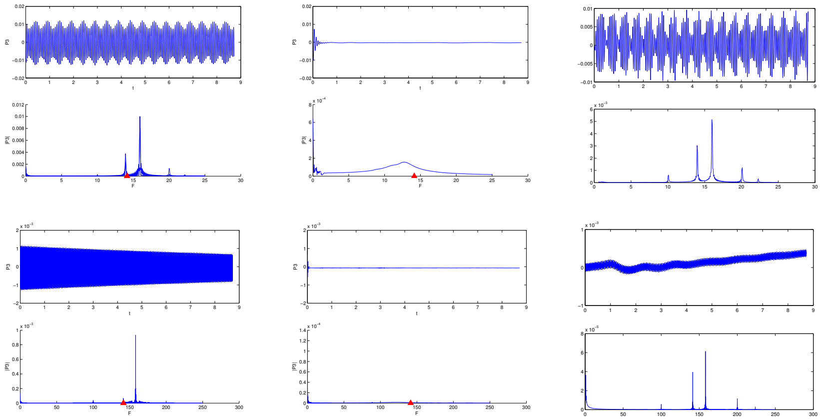

(a) VF CFL=0.5 (b) VF CFL=10 (c) PADE CFL=0.6

Figure: Acoustic pressure $P_3(0.66, 0.05, t)$ at $M_a = 0.1$ and $M_a = 0.01$

Influence of the preconditioning

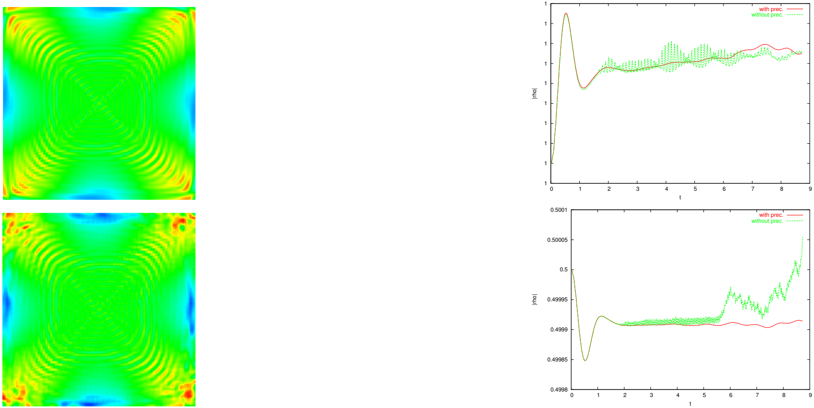

Figure: NadiaVF: influence of the preconditioning at $M_a = 0.1$ CFL=10 (80^2)

Viscous Taylor vortex at low Mach

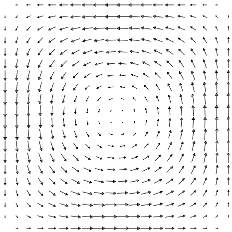

Parameters

- $Re = \frac{U_{max} L}{\nu} = 1000$
- $L = 1,\ U_{max} = 1,\ \rho_0 = 1,\ P_0 = \frac{M_a^{-2}}{\gamma}$

Compressible solution $\equiv$ inviscid + viscous decay

- mean thermodynamic part $\theta(M_a^{-2})$: $P_0 = \frac{M_a^{-2}}{\gamma}$
- unsteady incompressible part $\theta(1)$ (damped):
  $U(x,y,t) = U_2(x,y)\,e^{-2\nu\pi^2 t}$, $P(x,y,t) = P_2(x,y)\,e^{-4\nu\pi^2 t}$
- slow part $\theta(M_a^2)$: $\rho_2(x,y,\tau)$
- acoustic part $\theta(M_a)$(damped): $P_3(x,y,t)$

Numerical dissipation versus *h* and *Ma*

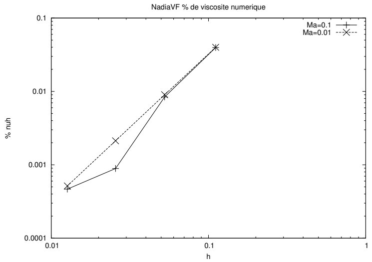

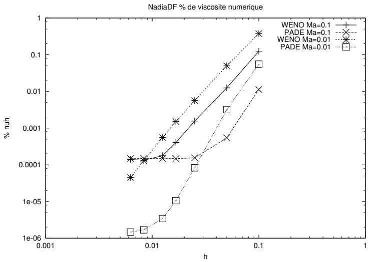

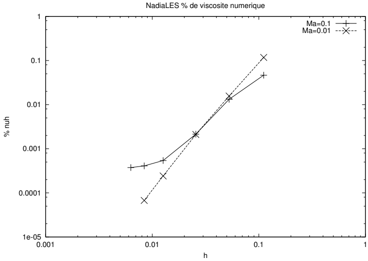

$$\frac{\|\rho U\|_{t=t_f}}{\|\rho U\|_{t=0}} = e^{-2\nu_e \pi^2 t_f}$$

$$\nu_e = \nu + \nu_h$$

Influence of the mesh on ρ_2 (slow part)

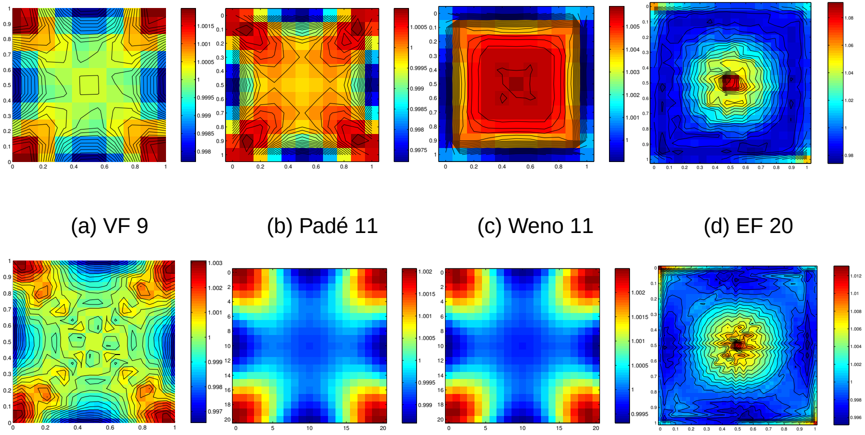

(a) VF 9 (b) Padé 11 (c) Weno 11 (d) EF 20

(e) VF 19 (f) Padé 21 (g) Weno 21 (h) EF 40

Compression of a Taylor vortex

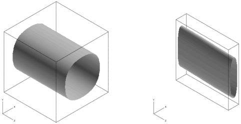

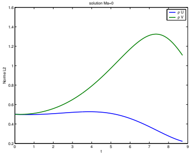

- model of the tumble in a combustion chamber

Parameters

$$Re = \frac{U_{max}L(0)}{\nu} = 1000 \text{ (stable)}$$
$$L(t) = 1 - \frac{V_p}{\omega} + \frac{V_p}{\omega}\sin\omega t$$
$$V_p = 0.144\,,\ \omega = 0, .36,\ T_c = 8.7$$

solution at $M_a = 0$

- compressed Taylor vortex
- $\rho_0(t) = \rho_0 \frac{L(0)}{L(t)}$, $P_0(t) = \frac{\rho_0(t)}{\gamma Ma^2}$
- acceleration of the v component
- viscous decay

Numerical solution

Evolution of the velocity norm at $Ma = 0.1$ and $Ma = 0.01$

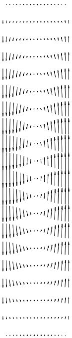

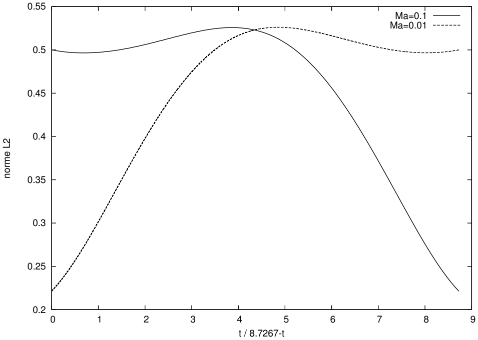

Velocity $U_2(x, y, t)$

All schemes predict the right velocity $U_2(x, y, t) \approx$ solution at $Ma = 0$

ρ_2 density fluctuation (slow part)

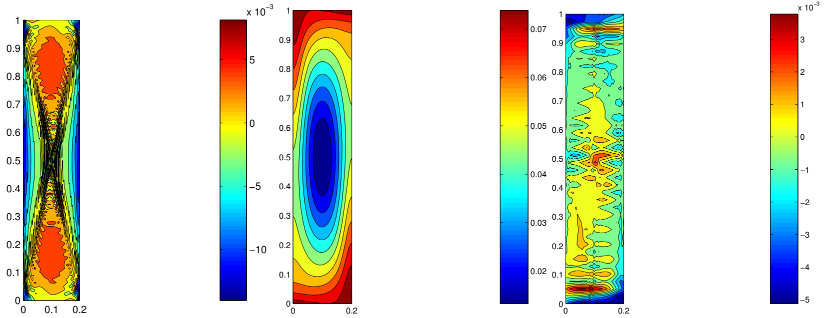

Figure: $\rho_2(x,y,T_c)$ at $Ma = 0.1$ (NadiaVF (animation), NadiaDF, NadiaLES)

	NadiaVF	NadiaWENO	NadiaPADE	NadiaLES
$Ma = 0.1$	$0.40\,10^{-1}$	$0.56\,10^{-1}$	$0.66\,10^{-1}$	$0.11\,10^{-1}$
$Ma = 0.01$	$0.41\,10^{-3}$	$0.44\,10^{-1}$	$0.29\,10^{-1}$	$0.97\,10^{-2}$

Table: maximum of the density fluctuation: $\rho_{max} - \rho_{min}$ at $t = T_c$ and 40^2

Acoustic

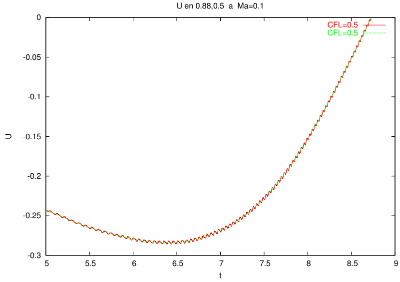

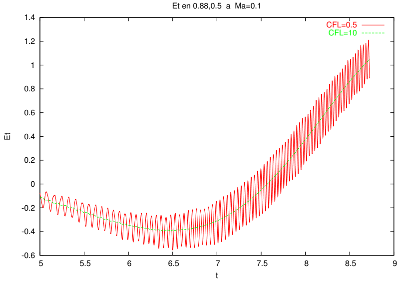

Figure: fluctuation at $(0.88, 0.5)$ (near the piston) of ρU and E_t at $M_a = 0.1$

The implicit scheme damp the acoustic if $CFL > 1$

acoustic waves are amplified by the compression

$\rightsquigarrow$pble with high order schemes

Computer cost of the schemes

	NadiaVF	NadiaPADE	NadiaWENO	NadiaLES
$Ma = 0.1$	837	6 357	6 355	17 216
$Ma = 0.01$	7686	58 712	58 706	156 000

Table: Number of time steps with the mesh 40^2

CPU time per iteration

- NadiaVF (Pentium IV 2.7 Ghz):$\approx 0.3s\,(Ma = 0.01)$ and $\approx 0.7s\,(Ma = 0.1)$
- NadiaDF (Pentium IV 1.7 Ghz) PADE: $\approx 0.04s$ and WENO:$\approx 0.07s$
- NadiaLES (Pentium IV 1.7 Ghz) maillage 3D $(3 * 40^2)$:$\approx 0.6s$

Perturbed 3D compression

- Spectral solution at $Ma = 0$ (Le Penven 2002)

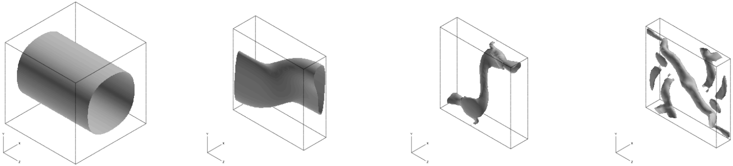

Figure: compression of a perturbed vortex at 1000 ($t = 0, 3, 5, 8$)

Numerical simulation

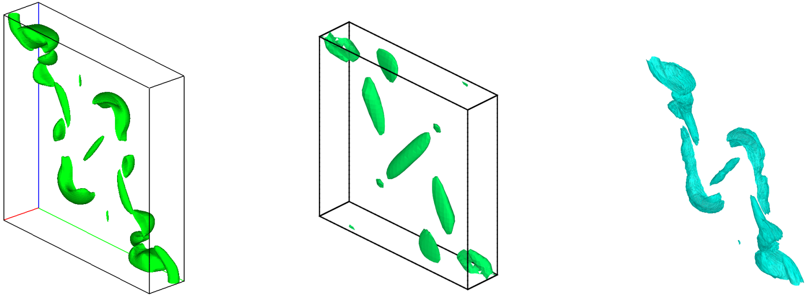

Figure: Iso-Vorticity at $t = T_c$ with NadiaVF, NadiaDF and NadiaLES

Animations of Iso Vorticity and Iso density ρ_2

Scheme properties (a)

All the schemes predict the "incompressible" ($M_a = 0$) part

NadiaVF (implicit center scheme): properties at low Mach

- needs preconditioning (stiff linear and non linear system)
- good prediction of the slow part even with CFL$>$ 1, with very small dissipation but some dispersion
- filtering of acoustic with CFL $>$ 1 and good prediction of the acoustic with CFL$<$ 1

Scheme properties (b)

NadiaDF (high order Padé and Weno schemes): properties at low Mach

- prediction of the slow part with some dissipation, but without dispersion
- precise schemes at $M_a = 0.1$, but need preconditioning at $M_a = 0.01$ for the acoustic

NadiaLES (mixed FV/FE Roe scheme): properties at low Mach

- robust code
- but least precise code
- needs fine mesh to get reasonable results for the slow part